Inorg. Chem. **2003**, *42*, 1187−1192

Magnetic Superstructures of Cupric Oxide CuO as Ordered Arrangements of One-Dimensional Antiferromagnetic Chains

H.-J. Koo and M.-H. Whangbo*

Department of Chemistry, North Carolina State University, Raleigh, North Carolina 27695-8204

Received September 23, 2002

In cupric oxide CuO, each Cu^{2+} ion has 12 nearest-neighbor Cu^{2+} ions grouped into six pairs related by inversion symmetry. The relative strengths of the Cu–O–Cu superexchange interactions in cupric oxide CuO were estimated by spin dimer analysis to confirm that the strongest superexchange interactions form one-dimensional antiferromagnetic chains along the [$10\bar{1}$] direction, and the remaining interactions are weak. We analyzed ordered arrangements of these one-dimensional antiferromagnetic chains to examine why the antiferromagnetic phase transition of CuO below 212.5 K adopts a (2a, b, 2c) superstructure. The local spin arrangement around each Cu^{2+} ion is more balanced in the ordered spin structures leading to a (2a, b, 2c) supercell than in any other ordered spin structures.

1. Introduction

The magnetic properties of cupric oxide CuO have been examined extensively in studies including magnetic susceptibility,[1−5] neutron diffraction,[6−8] neutron scattering,[9] NMR,[10−12] and specific heat measurements.[13] This attention to CuO resulted largely from the facts that many structural and magnetic properties of CuO resemble those of high-T_c cuprate superconductors, and that CuO exhibits unusual magnetic properties. The structural building blocks of cupric oxide are CuO_2 ribbon chains made up of edge-sharing CuO_4 square planar units. The three-dimensional lattice of CuO is constructed from these CuO_2 chains by oxygen corner-sharing (Figure 1a).[14] Because the ribbon planes of every two CuO_2 chains condensed by corner-sharing are not perpendicular to each other (Figure 1b), each Cu^{2+} site is connected to its 10 adjacent Cu^{2+} sites by four kinds of Cu−O−Cu superexchange paths [i.e., Cu(1)−O−Cu(2), Cu(1)−O−Cu(3), Cu(1)−O−Cu(4), and Cu(1)−O−Cu(5)] (Figure 1c). Each Cu^{2+} ion is surrounded by two additional Cu^{2+} ions unconnected by a Cu−O−Cu superexchange path (Figure 1a). The 12 Cu^{2+} ions around each Cu^{2+} ion are grouped into six pairs related by inversion symmetry.

As the temperature is increased above $T_{N1} = 231$ K, the magnetic susceptibility of CuO does not decrease according to the Curie−Weiss law, but increases, passes through a wide maximum at 540 K, and then diminishes.[1] Thus, CuO behaves as one-dimensional (1D) antiferromagnetic chains above T_{N1}. Below $T_{N1} = 231$ K, CuO becomes a three-dimensional collinear antiferromagnet with a magnetic moment 0.68 μ_B per Cu^{2+} ion,[6,9] which is considerably smaller than the pure spin value 1 μ_B. CuO undergoes a phase transition below T_{N1} to form an incommensurate antiferromagnetic structure with propagation vector (0.506, 0, −0.483). Below $T_{N2} = 212.5$ K, the latter is transformed into a commensurate antiferromagnetic structure with propagation

* To whom correspondence should be addressed. E-mail: mike_whangbo@ncsu.edu.

(1) O'Keeffe, M.; Stone, F. S. *J. Phys. Chem. Solids* **1962**, *23*, 261.
(2) Kondo, O.; Ono, M.; Sugiura, E.; Sugiyama, K.; Data, M. *J. Phys. Soc. Jpn.* **1988**, *57*, 3293.
(3) Köbler, U.; Chattopadhyay, T. *Z. Phys. B: Condens. Matter* **1991**, *82*, 383.
(4) Arbuzova, T. I.; Samokhvalov, A. A.; Smolyak, I. B.; Karpenko, B. V.; Chebotaev, N. M.; Naumov, S. V. *J. Magn. Magn. Mater.* **1991**, *95*, 168.
(5) Arbuzova, T. I.; Smolyak, I. B.; Samokhvalov, A. A.; Naumov, S. V. *J. Exp. Theor. Phys.* **1998**, *86*, 559.
(6) Forsyth, J. B.; Brown, P. J.; Wanklyn, B. M. *J. Phys. C: Solid State Phys.* **1988**, *21*, 2917.
(7) Brown, P. J.; Chattopadhyay, T.; Forsyth, J. B.; Nunez, V.; Tasset, F. *J. Phys. C: Condens. Matter* **1991**, *3*, 4281.
(8) Aïn, M.; Menelle, A.; Wanklyn, B. M.; Bertaut, E. F. *J. Phys. C: Condens. Matter* **1992**, *4*, 5327.
(9) Yang, B. X.; Thurston, T. R.; Tranquada, J. M.; Shirane, G. *Phys. Rev. B* **1989**, *39*, 4343.
(10) Tsuda, T.; Shimizu, T.; Yasuoka, H.; Kishio, K.; Kitazawa, K. *J. Phys. Soc. Jpn.* **1988**, *57*, 2908.
(11) Ziolo, J.; Borsa, F.; Corti, M.; Rigamonti, A.; Parmigiani, F. *J. Appl. Phys.* **1990**, *67*, 5864.
(12) Shimizu, T.; Matsumoto, T.; Goto, A.; Yoshimura, K.; Kosuge, K. *Physica B* **1999**, *259*−*261*, 573.
(13) Loram, J. W.; Mirza, K. A.; Joyce, C. P.; Osborne, A. J. *Europhys. Lett.* **1989**, *8*, 263.
(14) Åsbrink, S.; Norrby, L.-J. *Acta Crystallogr., Sect. B* **1970**, *26*, 8.

10.1021/ic020576k CCC: $25.00
Published on Web 01/23/2003

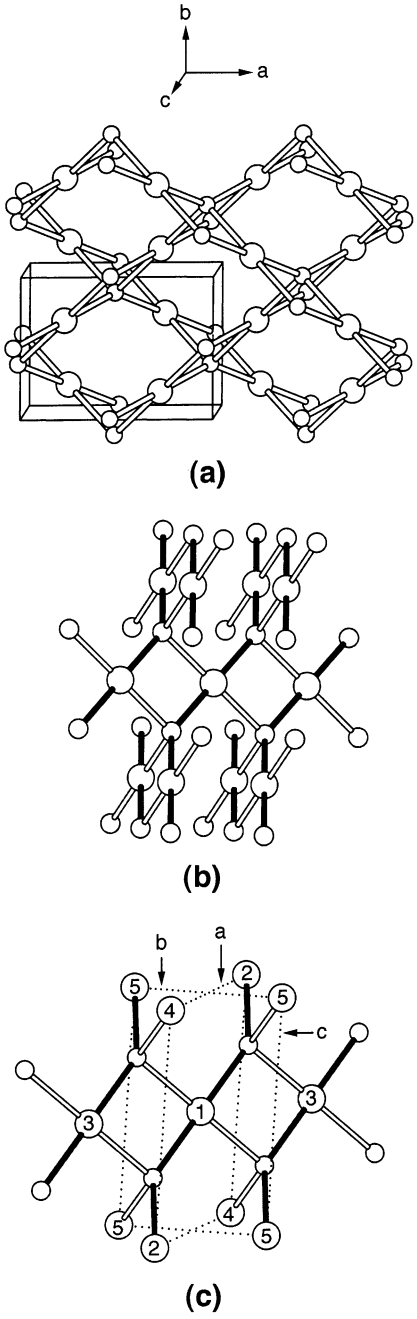

Figure 1. (a) Perspective view of corner-sharing CuO_2 ribbon chains in cupric oxide CuO. (b) Zoomed-in view of corner-sharing CuO_2 ribbon chains. (c) Zoomed-in view of a CuO_2 ribbon chain showing the unit cell vector directions. The strongly interacting Cu−O−Cu superexchange paths are presented by filled cylinders.

vector (0.5, 0, −0.5).[6,9] Thus, the magnetic phase transition below T_{N2} doubles the unit cell along the *a*- and *c*-directions. It has been identified that the strongest antiferromagnetic interactions between the adjacent Cu^{2+} ions of CuO occur along the $[10\bar{1}]$ direction through the superexchange paths having the largest ∠Cu−O−Cu angle (i.e., 145.8°), i.e., Cu(1)−O−Cu(2). (In Figure 1b,c, the Cu−O bonds representing these paths are indicated by filled cylinders.) This is understandable according to Goodenough rules for superexchange interaction.[15] The spin exchange parameter $|J|$ for these 1D antiferromagnetic chains was estimated to be 67 ± 20 meV from the spin-wave velocity $v = |J|d = 250 \pm 75$ using the distance d between the nearest neighbor Cu^{2+} ions along the $[10\bar{1}]$ direction (i.e., 3.75 Å).[9] This agrees well with the value of 73 meV[12] estimated from the relationship $|J| = 1.560k_BT_{max}$[16] for the magnetic susceptibility of a 1D antiferromagnetic Heisenberg chain using $T_{max} = 540$ K,[1] where T_{max} is the temperature at which the magnetic susceptibility is maximum. The $|J|$ value of CuO is approximately half that estimated for La_2CuO_4 (i.e., 115 meV).[17]

Table 1. Geometrical Parameters and $(\Delta e)^2$ Values Associated with the Four Superexchange Paths Cu(1)−O−Cu(j) (j = 2−5) of CuO[a,b]

path	Cu···Cu	Cu−O	∠Cu−O−Cu	$-(\Delta e)^2$	$-J_{AF}$
$j = 2$	3.749	1.961, 1.961	145.8	51500	73
$j = 3$	2.901	1.961, 1.951	95.7	3360	4.8
$j = 4$	3.173	1.951, 1.951	108.9	1160	1.6
$j = 5$	3.083	1.951, 1.961	104.0	360	0.5

[a] The distances in Å units, and the angles in deg. [b] The $-(\Delta e)^2$ values are in units of $(meV)^2$, and the $-J_{AF}$ values in units of meV.

A structural motif and magnetic properties similar to those of CuO are also found for paramelaconite Cu_4O_3.[18,19] The Cu_2O_3 lattice of Cu^{2+} ions, which results from Cu_4O_3 by removing the diamagnetic Cu^+ ions, is made up of corner-sharing CuO_2 ribbon chains. The magnetic susceptibility of Cu_4O_3 shows a maximum around 75 K and a sharp decrease below 42.3 K.[19] The magnetic phase transition below 42.3 K leads to a supercell (2a, 2b, 2c);[19] i.e., it doubles the unit cell along each crystallographic direction. Recently, we have shown[20] that the magnetic properties of Cu_4O_3 and its isostructural analogue $Ag_2Cu_2O_3$[21−23] are well explained on the basis of the relative strengths of their Cu−O−Cu superexchange interactions estimated by spin dimer analysis.

The spin exchange interactions between the 1D antiferromagnetic chains of CuO have been regarded as weak because the associated ∠Cu−O−Cu angles are much closer to 90° than to 180° (Table 1). To a first approximation, therefore, the incommensurate and commensurate magnetic superstructures of CuO are ordered structures of the 1D antiferromagnetic chains. Nevertheless, it is not well understood whether an ordering of the 1D antiferromagnetic chains gives rise to other magnetic superstructures equally probable as the (2a, 0, 2c) superstructure and whether the interactions

(15) Goodenough, J. B., *Magnetism and the Chemical Bond*; Wiley: Cambridge, MA, 1963.
(16) Kahn, O. *Molecular Magnetism*; VCH Publishers: Weinheim, 1993.
(17) Shirane, G.; Endoh, Y.; Birgeneau, R. J.; Kastner, M. A.; Hidaka, Y.; Oda, M.; Suzuki, M.; Murakami, T. *Phys. Rev. Lett.* **1987**, *59*, 1613.
(18) O'Keeffe, M.; Bovin, J.-O. *Am. Mineral.* **1978**, *63*, 180.
(19) Pinsard-Gaudart, J.; Rodriguez-Carvajal, J.; Gukasov, A.; Monod, P.; Dechamps, M.; Jegoudez, J. Propriétés magnétiques de Cu_4O_3-Un reseau pyrochlore à spin 1/2. Presented at Colloque Oxydes à Propriétés Remarquables: Ordre de spins, ordre de charges et phénomènes coopératifs, organized by Berthier, C., Collin, G., Doumerc, J.-P.; Bombannes, June 6−8, 2001. The abstracts of the meeting are collected in the Report GDR 2069.
(20) Whangbo, M.-H.; Koo, H.-J. *Inorg. Chem.* **2002**, *41*, 3570 and the references therein.
(21) Gómez-Romero, P.; Tejada-Rosales, E. M.; Palacín, M. R. *Angew. Chem., Int. Ed.* **1999**, *38*, 524.
(22) Adelsberger, K.; Curda, J.; Vensky, S.; Jansen, M. *J. Solid State Chem.* **2001**, *158*, 82.
(23) Tejada-Rosales, E. M.; Rodriguez-Carvajal, J.; Palacin, M. R.; Gómez-Romero, P. *Mater. Sci. Forum* **2001**, *378*−*381*, 606.

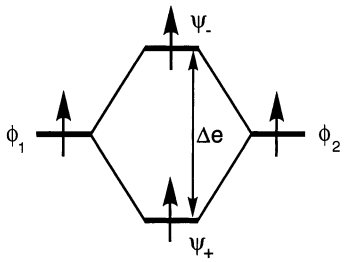

Figure 2. Orbital interaction diagram between two magnetic sites in a spin dimer, where the spin−orbital interaction energy Δe is defined as the energy difference of the two singly filled orbitals of the spin dimer.

between the 1D antiferromagnetic chains possess any energetic or statistical factor favoring the (2a, 0, 2c) superstructure. In the present work, we probe these questions by evaluating the relative strengths of the various Cu−O−Cu superexchange interactions of CuO on the basis of spin dimer analysis and then analyzing possible orderings between the 1D antiferromagnetic chains that double the unit cell along the *a*-, *b*-, and *c*-directions.

2. Spin Dimer Analysis

The strengths of spin exchange interactions (i.e., spin exchange parameters *J*) in an extended magnetic solid can be determined by performing electronic structure calculations for the high- and low-spin states of spin dimers (i.e., structural units consisting of two spin sites)[24−26] or electronic band structure calculations for various ordered spin arrangements of a magnetic solid.[27] In understanding physical properties of magnetic solids, it is often sufficient to estimate the relative magnitudes of their *J* values on the basis of tight-binding electronic structure calculations.[16,20,28−30] In general, a spin exchange parameter *J* is written as $J = J_F + J_{AF}$, where the ferromagnetic term J_F (>0) is small so that the spin exchange becomes ferromagnetic (i.e., $J > 0$) when the antiferromagnetic term J_{AF} (<0) is negligibly small in magnitude. Spin exchange interactions of magnetic solids are mostly antiferromagnetic (i.e., $J < 0$) and can be discussed by focusing on the antiferromagnetic terms, J_{AF}.[16,20,28−30]

Suppose that each spin site of a magnetic solid contains one unpaired electron, the two spin sites of a spin dimer are equivalent, and the two spin sites of a spin dimer are represented by nonorthogonal magnetic orbitals (i.e., singly occupied molecular orbitals of the spin monomers) ϕ_1 and ϕ_2. If Δe is the spin−orbital interaction energy (Figure 2) between ϕ_1 and ϕ_2, then the antiferromagnetic term J_{AF} is related to Δe as[16,20,28,29,31]

$$J_{AF} = -(\Delta e)^2/U_{eff} \quad (1)$$

where U_{eff} is the effective on-site repulsion. For a set of closely related magnetic solids, the U_{eff} value would be nearly constant and hence could be used to approximate antiferromagnetic *J* by $-(\Delta e)^2$.[20,30]

In calculating the Δe values for various spin exchange paths of the CuO lattice, it is necessary to specify the corresponding spin dimers. Within each CuO_2 ribbon chain, the spin dimer for the nearest-neighbor interaction is the edge-sharing dimer Cu_2O_6. Between adjacent corner-sharing CuO_2 ribbon chains, the spin dimer for the nearest-neighbor interaction is the corner-sharing dimer Cu_2O_7. Table 1 summarizes some geometrical parameters associated with the spin dimers of CuO.[14]

In describing the spin exchange interactions of magnetic solids in terms of Δe values obtained from extended Hückel molecular orbital calculations,[32,33] it is found necessary[20,29,30] to employ double-ζ Slater type orbitals (STOs)[34] for both the d orbitals of the transition metal and the s/p orbitals of the surrounding ligand atoms. The atomic orbital parameters of Cu and O employed for our calculations are summarized in Table 2. The Δe values are affected most sensitively by the exponent ζ' of the diffuse STO of the O 2p orbital. Our studies[20,30] on other magnetic solids show that the ζ' value appropriate for studying spin exchange interactions of magnetic oxides should be increased from that of Clementi and Roetti[34] by 10−13%. The ζ' values of the O 2p orbitals listed in Table 2 are those increased by 12.5%.

Table 2. Exponents ζ_i and Valence Shell Ionization Potentials H_{ii} of Slater-Type Orbitals χ_i Used for Extended Hückel Tight-Binding Calculation[a]

atom	χ_i	H_{ii} (eV)	ζ_i	C_i[b]	ζ'_i	C_i[b]
Cu	4s	−11.4	2.151	1.0		
Cu	4p	−6.06	1.370	1.0		
Cu	3d	−14.0	7.025	0.4473	3.004	0.6978
O	2s	−32.3	2.688	0.7076	1.675	0.3745
O	2p	−14.8	3.694	0.3322	1.866	0.7448

[a] H_{ii}'s are the diagonal matrix elements $\langle\chi_i|H^{eff}|\chi_i\rangle$, where H^{eff} is the effective Hamiltonian. In our calculations of the off-diagonal matrix elements $H_{ij} = \langle\chi_i|H^{eff}|\chi_j\rangle$, the weighted formula was used. See: Ammeter, J.; Bürgi, H.-B.; Thibeault, J.; Hoffmann, R., *J. Am. Chem. Soc*. **1978**, *100*, 3686. [b] Coefficients used in the double-ζ Slater-type orbital expansion.

3. Relative Strengths of Spin Exchange Interactions

The $(\Delta e)^2$ values calculated for the four superexchange interactions of CuO are listed in Table 1, where the corresponding J_{AF} values were calculated by using eq 1 with $U_{eff} = 705$ meV. This U_{eff} value reproduces the *J* value of −73 meV for the 1D antiferromagnetic chain made up of

(24) Illas, F.; Moreira, I. de P. R.; de Graaf, C.; Barone, V. *Theor. Chem. Acc.* **2000**, *104*, 265 and the references therein.
(25) Noodleman, L. *J. Chem. Phys.* **1981**, *74*, 5737.
(26) Dai, D.; Whangbo, M.-H. *J. Chem. Phys*. **2001**, *114*, 2887; **2003**, *118*, 29.
(27) Derenzo, S. E.; Klitenberg, M. K.; Weber, M. J. *J. Chem. Phys*. **2000**, *112*, 2074 and the references therein.
(28) Hay, P. J.; Thibeault, J. C.; Hoffmann, R. *J. Am. Chem. Soc*. **1975**, *97*, 4884.
(29) Dai, D.; Koo, H.-J.; Whangbo, M.-H. In *Solid State Chemistry of Inorganic Materials III*; Geselbracht, M. J., Greedan, J. E., Johnson, D. C., Subramanian, M. A., Eds.; MRS Symposium Proceedings, Vol. 658; Materials Research Society: Warrendale, PA, 2001; GG5.3.1−5.3.11 and the references therein.
(30) Koo, H.-J.; Whangbo, M.-H.; VerNooy, P. D.; Torardi, C. C.; Marshall, W. J. *Inorg. Chem*. **2002**, *41*, 4664 and the references therein.
(31) This expression is valid when spin exchange parameters of a spin Hamiltonian are written as *J* instead of 2*J*.
(32) Hoffmann, R. *J. Chem. Phys*. **1963**, *39*, 1397.
(33) Our calculations were carried out by employing the *CAESAR* program package (Ren, J.; Liang, W.; Whangbo, M.-H. *Crystal and Electronic Structure Analysis Using CAESAR*; 1998; http://www.PrimeC.com/).
(34) Clementi, E.; Roetti, C. *At. Data Nucl. Data Tables* **1974**, *14*, 177.

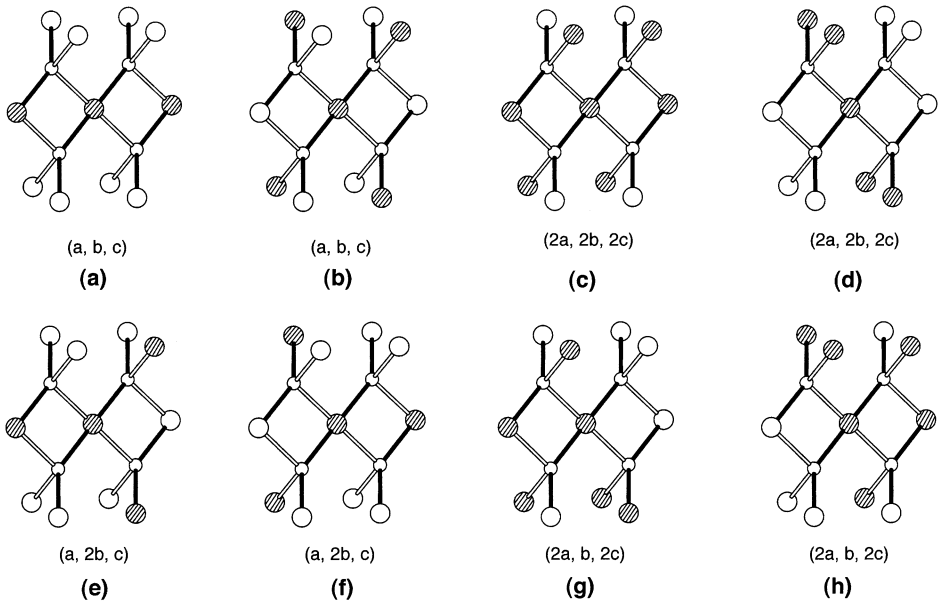

Figure 3. Eight possible spin arrangements in the 10 Cu^{2+} ions connected, by superexchange paths, to a given Cu^{2+} ion. The up-spin and down-spin Cu^{2+} sites are indicated by shaded and unshaded circles, respectively. For convenience, the central Cu^{2+} ion is assumed to have an up-spin. The arrangements a and b retain the chemical unit cell (a, b, c). The arrangements c and d lead to a (2a, 2b, 2c) supercell, the arrangements e and f to a (a, 2b, c) supercell, and the arrangements g and h to a (2a, b, 2c) supercell.

the Cu(1)−O−Cu(2) paths. As expected, the antiferromagnetic exchange interaction through the Cu(1)−O−Cu(2) path is by far the strongest. The second strongest antiferromagnetic exchange interaction occurs through the Cu(1)−O−Cu(3) paths. The remaining two superexchange paths Cu(1)−O−Cu(4) and Cu(1)−O−Cu(5) provide much weaker antiferromagnetic interactions. It is noted that the Cu(1)−O−Cu(3) path has a smaller ∠Cu−O−Cu angle than do Cu(1)−O−Cu(4) and Cu(1)−O−Cu(5) (i.e., 95.7° vs 108.9° and 104.0°), but it provides a stronger antiferromagnetic interaction. The Cu(1) and Cu(3) atoms are connected by two Cu−O−Cu bridges. In contrast, the Cu(1) and Cu(4) atoms are connected by a single Cu−O−Cu bridge, and so are the Cu(1) and Cu(5) atoms.

For the Cu−O−Cu superexchange interaction of La_2CuO_4, the J_{AF} value is estimated to be −145 meV from our calculation of $(\Delta e)^2$ using $U_{eff} = 705$ meV. The Cu−O−Cu superexchange path of La_2CuO_4[35] has a shorter Cu−O bond length (i.e., 1.907 Å) and a larger ∠Cu−O−Cu angle (i.e., 174.5°) than does the strongest superexchange path of CuO (i.e., Cu−O = 1.961 Å and ∠Cu−O−Cu = 145.8°). Consequently, the antiferromagnetic superexchange interaction is much stronger in La_2CuO_4 than in CuO. It should be noted that the J_{AF} value of −145 meV is not far from the J value of −115 meV estimated experimentally.[9] Thus, it is expected that the relative strengths of the spin exchange interactions of CuO determined from the calculated $(\Delta e)^2$ values are reliable.

4. Ordering of the One-Dimensional Antiferromagnetic Chains

It is important to investigate what possible commensurate magnetic superstructures of CuO result from ordering of 1D antiferromagnetic chains. For simplicity, we limit our discussion to those orderings that either keep the chemical unit cell (*a*, *b*, *c*) or double the unit cell along the *a*-, *b*-, or *c*-direction. With this restriction, there are only eight different ways of ordering the 1D antiferromagnetic chains surrounding a given 1D antiferromagnetic chain (Figure 3a−h). The two spin arrangements of Figure 3a,b retain the chemical unit cell. The ordered spin structure of Figure 4a results from the spin arrangement of Figure 3a, and that of Figure 4b results from the spin arrangement of Figure 3b. The two spin arrangements of Figure 3c,d lead to a supercell (2a, 2b, 2c). The ordered spin structure of Figure 4c is obtained from the spin arrangements of Figure 3c,3d. The two spin arrangements of Figure 3e,f give rise to a supercell (a, 2b, c). The ordered spin structure of Figure 4d results from the spin arrangements of Figure 3e,f. Finally, a supercell (2a, b, 2c) is derived from the spin arrangements of Figure 3g,h. The ordered spin structure of Figure 4e is obtained from the patterns of Figure 3g,h.

5. Discussion

Table 1 shows that the three Cu(1)−O−Cu(*j*) (*j* = 3−5) superexchange interactions, which control the interactions between the 1D antiferromagnetic chains, are weak. Thus, one might speculate that the three interchain superexchange interactions can be either weakly ferromagnetic or weakly antiferromagnetic. Then, all the eight possible spin arrangements of Figure 3a−h are equally probable. This leads to the prediction that, at temperatures below T_{N2}, a unit doubling should be observed not only along the *a*- and *c*-directions due to the spin arrangements c, d, g, and h, but also along the *b*-direction due to the spin arrangements c, d, e, and f. The latter prediction is inconsistent with the results of the available experiments.[6−9] Consequently, it is necessary to

(35) Grande, B.; Müller-Buschbaum, Hk.; Schweitzer, M. *Z. Anorg. Allg. Chem*. **1977**, *428*, 120.

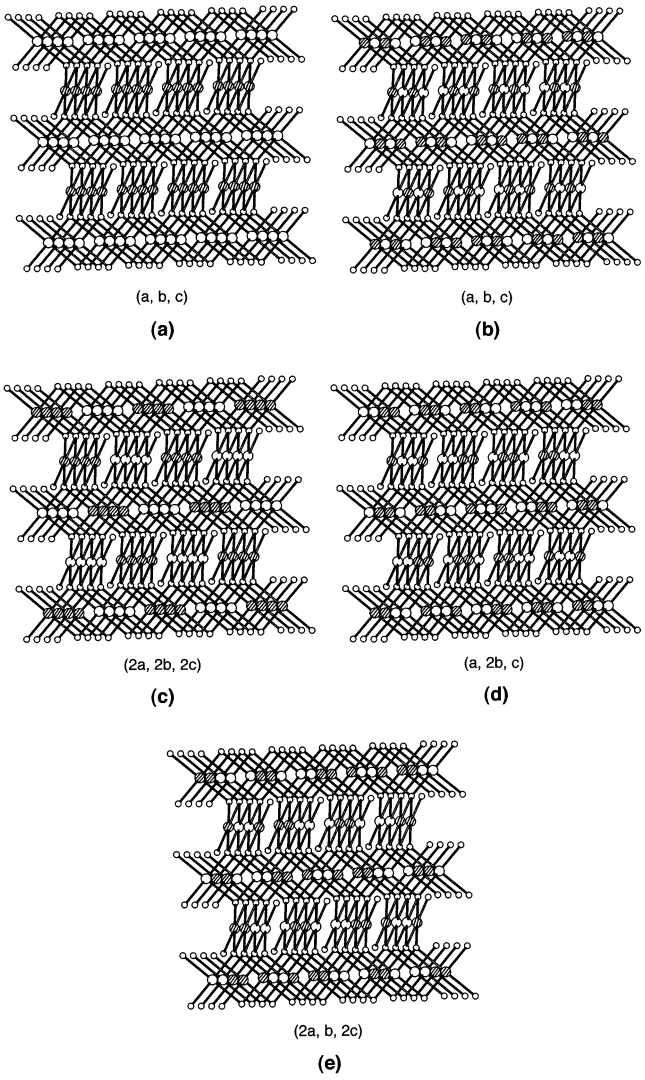

Figure 4. Ordered spin structures derived from the eight possible spin arrangements shown in Figure 3a−h: (a) from the pattern of Figure 3a, (b) from the pattern of Figure 3b, (c) from the patterns of Figure 3c,d, (d) from the patterns of Figures 3e,f, and (e) from the patterns of Figures 3g,h.

Table 3. Nature of the Spin Ordering along the Cu(1)−O−Cu(j) (j = 2−5) Spin Exchange Paths in Cupric Oxide CuO

		Cu(1)−O−Cu(j)[b]			
case[a]	superstructure	$j = 2$	$j = 3$	$j = 4$	$j = 5$
a	(a, b, c)	AFM	FM	AFM	AFM
b	(a, b, c)	AFM	AFM	AFM	FM
c, d	(2a, 2b, 2c)	AFM	AFM, FM	FM	AFM, FM
e, f	(a, 2b, c)	AFM	$(\uparrow\uparrow\downarrow\downarrow)_\infty$	AFM	$(\uparrow\uparrow\downarrow\downarrow)_\infty$
g, h	(2a, b, 2c)	AFM	$(\uparrow\uparrow\downarrow\downarrow)_\infty$	FM	$(\uparrow\uparrow\downarrow\downarrow)_\infty$

[a] These cases refer to those listed in Figure 3. [b] The Cu(1)−O−Cu(j) superexchange paths are defined in Figure 1c. The symbols AFM and FM mean antiferromagnetic and ferromagnetic arrangements, respectively.

consider that there exists an energetic factor favoring the spin arrangements g and h over the spin arrangements a−f.

Table 3 summarizes the nature of the long-range spin ordering along the directions of the Cu(1)−O−Cu(2), Cu(1)−O−Cu(3), Cu(1)−O−Cu(4), and Cu(1)−O−Cu(5) spin exchange paths in the ordered spin structures of Figure 4a−e. From the consideration of these long-range spin orders, it is not clear why CuO prefers the ordered spin structures

Table 4. Local Spin Distributions around Cu^{2+} Ions in the Ordered Spin Structures of CuO that Result from the Ordering of 1D Antiferromagnetic Chains

case[a]	superstructure	spin distribution[b]	N_{CSP}[c]	N_{NCSP}[c]
a	(a, b, c)	↑: (4↑, 8↓)	0	5
		↓: (8↑, 4↓)	0	5
b	(a, b, c)	↑: (4↑, 8↓)	0	5
		↓: (8↑, 4↓)	0	5
c, d	(2a, 2b, 2c)	↑: (6↑, 6↓)	0	5
		↓: (6↑, 6↓)	0	5
e, f	(a, 2b, c)	↑: (4↑, 8↓)	4	1
		↓: (8↑, 4↓)	4	1
g, h	(2a, b, 2c)	↑: (6↑, 6↓)	4	1
		↓: (6↑, 6↓)	4	1

[a] These cases are defined in Figure 3. [b] The notations are defined as follows: for example, ↑: (m↑, n↓) means that the 12 spins surrounding each up-spin Cu^{2+} site divided into m up-spins and n down-spins. [c] N_{CSP} refers to the number of compensating spin pairs, and N_{NCSP}, the number of noncompensating spin pairs.

leading to the (2a, b, 2c) supercell over the other ordered spin structures. Thus, we analyze the local spin distributions around each spin site. As already pointed out, each Cu^{2+} ion is surrounded by 12 nearest-neighbor Cu^{2+} ions grouped into six pairs of Cu^{2+} ions related by inversion symmetry at the central Cu^{2+} ion. The 10 nearest-neighbor Cu^{2+} ions that are not involved in making a 1D antiferromagnetic chain with the central Cu^{2+} ion lie within the narrow distance range 2.90−3.17 Å (Figure 1, Table 1). It is of interest to see how up-spins and down-spins are distributed among the 12 nearest-neighbor spin sites surrounding each spin site. Table 4 summarizes these local spin distributions in the ordered spin structures derived from the eight spin arrangements a−h of Figure 3. The 12 Cu^{2+} ions surrounding each Cu^{2+} ion are divided into equal numbers of up-spin and down-spin ions in the ordered spin structures leading to the (2a, b, 2c) and (2a, 2b, 2c) supercells, but into unequal numbers of up-spin and down-spin ions in the ordered spin structures leading to the (a, 2b, c) supercell or retaining the chemical unit cell (a, b, c). Thus, in terms of the numbers of up-spin and down-spin ions around each spin site, the local spin arrangement around each Cu^{2+} ion is balanced only in the ordered spin structures leading to the (2a, b, 2c) and (2a, 2b, 2c) supercells.

To further distinguish the ordered spin structures possessing the unit cells (a, b, c), (a, 2b, c), (2a, b, 2c), and (2a, 2b, 2c), we examine the nature of spin distribution in each pair of spin sites related by inversion symmetry at each Cu^{2+} site. Of the six pairs of spin sites surrounding each spin site, one pair is used to form a 1D antiferromagnetic chain with the central Cu^{2+} ion. Thus, only the spin arrangements in the remaining five pairs are important for the interchain interactions. In each of these five pairs, the two spins can be either opposite (i.e., compensating) or identical (i.e., noncompensating). The number of compensating spin pairs (N_{CSP}) and that of noncompensating spin pairs (N_{NCSP}) around each spin site in the ordered spin structures of Figure 4a−e are summarized in Table 4. The spin distribution around each spin site is more balanced when N_{CSP} is larger. Thus, in terms of the number of compensating spin pairs around each spin site, the local spin arrangement around each Cu^{2+} ion is much better balanced in the ordered spin structures leading to the

unit cells (2a, b, 2c) and (a, 2b, c) supercells than in those leading to the unit cells (a, b, c) and (2a, 2b, 2c).

This discussion reveals that the local spin arrangement around each Cu^{2+} ion is most balanced in the ordered spin structures leading to the unit cells (2a, b, 2c) both in terms of the numbers of up-spins and down-spins around each spin site and in terms of the number of compensating spin pairs around each spin site. The experimental observation of the (2a, b, 2c) supercell below T_{N2} leads us to conclude that such a balanced local spin distribution around a spin site with inversion symmetry is energetically favorable. If this factor is weak, it would be possible to observe weak magnetic reflection peaks corresponding to the (a, 2b, c) and (2a, 2b, 2c) supercells.

6. Concluding Remarks

Our spin dimer analysis confirms that the Cu−O−Cu superexchange paths with the largest ∠Cu−O−Cu angle have the strongest antiferromagnetic interactions thereby forming 1D antiferromagnetic chains along the $[10\bar{1}]$ direction, and the interactions between these 1D antiferromagnetic chains are weak. Thus, the magnetic superstructures of CuO can be viewed as ordered structures of the 1D antiferromagnetic chains. Our analysis of the local spin arrangements in ordered spin structures possessing the unit cells (a, b, c), (a, 2b, c), (2a, b, 2c), and (2a, 2b, 2c) reveals that the local spin arrangement around each Cu^{2+} ion is most balanced in the ordered spin structures leading to the unit cells (2a, b, 2c) both in terms of the numbers of up-spins and down-spins around each spin site and in terms of the number of compensating spin pairs around each spin site. From the experimental observation of the (2a, b, 2c) supercell below T_{N2}, it is concluded that such a balanced local spin distribution around a spin site with inversion symmetry is energetically favorable.

Acknowledgment. The work at North Carolina State University was supported by the Office of Basic Energy Sciences, Division of Materials Sciences, U.S. Department of Energy, under Grant DE-FG02-86ER45259.

IC020576K